

Article

Effect of the Solvent on the Basic Properties of Mg–Al Hydrotalcite Catalysts for Glucose Isomerization

Suna An, Dahye Kwon, JeongHyun Cho and Ji Chul Jung *

Department of Chemical Engineering, Myongji University, Yongin 17058, Korea; suna960312@gmail.com (S.A.); kdahye829@gmail.com (D.K.); po78jhjh@gmail.com (J.C.)

* Correspondence: jchung@mju.ac.kr

Received: 5 October 2020; Accepted: 23 October 2020; Published: 25 October 2020



Abstract: We suggested the existence of a relationship between the base properties of Mg–Al hydrotalcite catalysts and the solvents employed in the industrially important isomerization of glucose produce fructose. We prepared Mg–Al hydrotalcite catalysts with different Mg/Al atomic ratios to tune the basic properties of the catalyst. The prepared catalysts were used in the glucose isomerization conducted in various solvents. Experimental results confirmed that the catalysts exhibited different activities in the different solvents. We also implemented the Hammett indicator method, which allows to analyze the basic properties of the catalysts in various solvents. According to evidence, the basic properties of the catalysts varied substantially in different solvents. Notably, increases in the catalysts' base properties matched the observed increases in fructose yield of the glucose isomerization. Consequently, we suggested that, in order to prepare efficient Mg–Al hydrotalcite catalysts for glucose isomerization, the interaction between the solvent used to conduct the reaction and the basic properties of the catalyst, which are in turn influenced by the solvent, should be considered.

Keywords: solvent; base property; glucose isomerization; Mg–Al hydrotalcite; Mg/Al atomic ratio

1. Introduction

The term biomass refers to plants that synthesize organic matter by exploiting solar energy and biological organisms, such as animals and microorganisms, which use plants as food. Biomass is abundantly present in nature, and, because of its eco-friendly properties, it is increasingly attracting the attention of researchers as a promising sustainable energy source [1–9]. In particular, carbohydrates derived from biomass are the focus of considerable research interest as a resource that can be converted into valuable compounds [10–13]. The most abundant and inexpensive of carbohydrates, glucose, can be obtained by acid-saccharification or enzymatic saccharification of starch and cellulosic. Glucose can in turn be converted into the expensive carbohydrate fructose through an isomerization assisted by a base catalyst. Fructose is easily switchable not only with dietary sugar for food applications, but with useful substances such as 5-hydroxymethylfurfural (HMF) and levulinic acid [14]. Therefore, a reaction for producing fructose from glucose has been in the limelight, and studies on this transformation have been actively promoted [15–20].

The isomerization of glucose to fructose is known to be possible using biological enzymes or chemically inorganic catalysts [21,22]. In practice, catalyzing the mentioned isomerization with enzymes requires high-purity glucose as a reactant, and it has a disadvantage that its process operating temperature needs to remain in a narrow window [14]. However, glucose isomerization effected via chemical means using an inorganic catalyst has multiple advantages: its operating temperature is not limited in comparison with the corresponding enzymatic process and has a long life. Indeed, base catalysts such as hydrotalcite, NaOH, and KOH are well known to be effective catalysts of the chemical isomerization of glucose to produce fructose. For this reason, studies on

glucose isomerization using the base catalysts have actively been conducted [23–26]. Therefore, in this study, we examined the use of base catalysts for glucose isomerization.

Glucose isomerization over base catalysts has been reported to generally follow the mechanism (Figure 1). Initially, glucose ring-opening takes place, so that the substrate assumes an open-chain structure [27]. Afterwards, glucose isomerization occurs, whereby fructose is generated via the Lobry de Bruyn-Alberda van Ekenstein (LdB-AvE) mechanism [28,29]. According to this mechanism, C2 protons are first extracted from glucose by a base catalyst to produce an intermediate. Subsequently, a proton is transferred from O2 to O1, and fructose is produced due to the protonation of C1. In some studies, the ring-opening of glucose has been influenced by the solvent [30,31]. In addition, the basic properties of the catalyst used in the reaction have been reported to play an important role in the glucose isomerization [32,33]. Therefore, many studies have been conducted on the effect of the basic properties of the catalyst on glucose isomerization; a number of reports have also been published on the effects of individual properties of the solvent on the said reaction [31,34,35]. In fact, most of the published studies have focused either on the effect of the solvent or on those of the catalyst on the reaction whereby fructose is obtained from glucose isomerization. However, the proposed overall mechanism of glucose isomerization suggests that the effect of the solvent on glucose ring-opening and the correlation between the basic properties of the catalyst by the solvent for the isomerization should be evaluated concomitantly. Therefore, we suggested the validity of investigating the interaction between the solvent and the catalyst, and not simply the individual characteristics of the solvent and the catalyst, as an approach to increasing the efficiency of glucose isomerization.

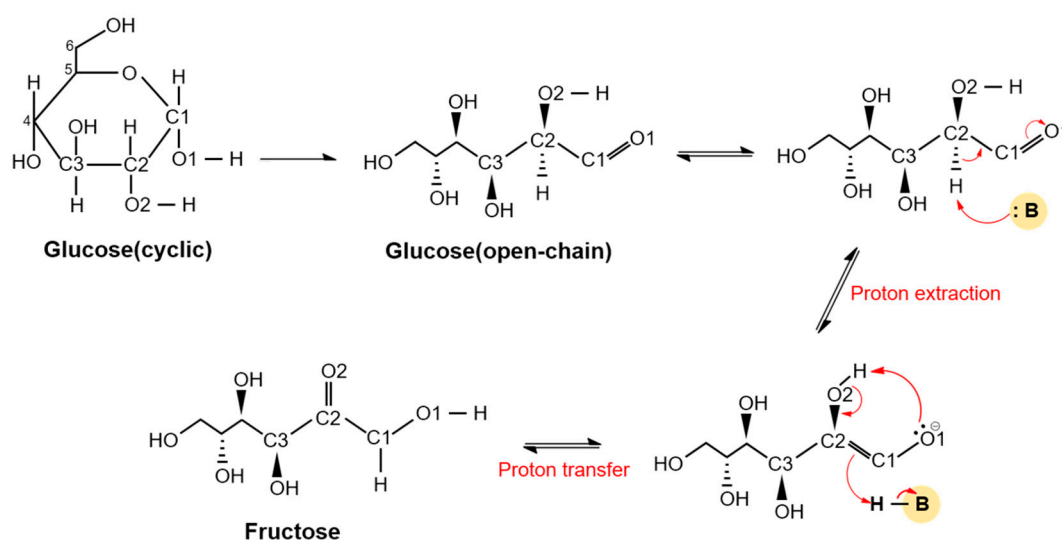


Figure 1. Mechanism of glucose ring-opening and isomerization over base catalysts.

Hydrotalcite (HT) has been widely studied as catalyst of glucose isomerization, and we selected it as a model catalyst in the present study. HT is characterized by a layered structure, and it has been widely used as an efficient catalyst for various base catalytic reactions [36–39]. In general, HT is known to have a chemical composition of $[\text{M}_{1-x}^{2+}\text{M}_x^{3+}(\text{OH})_2][\text{A}_{x/n}^{n-}\cdot m\text{H}_2\text{O}]$ [40–42]. Mg–Al HT, whereby the M^{2+} and M^{3+} sites are filled by Mg and Al cations, respectively, is a representative HT. The basic properties of Mg–Al HT can be controlled through various methods [43,44]. In particular, an easy way to control such properties is to tune the atomic Mg/Al atomic ratio in Mg–Al HT, and many studies have been published in which the Mg/Al ratio was made to vary [44,45].

In this study, we prepared four Mg–Al HT catalysts characterized by different Mg/Al atomic ratios. We then used these species to catalyze glucose isomerization, which was conducted in different reaction solvents (two protic solvents and two aprotic solvents). We observed that catalysts with different Mg/Al atomic ratios displayed different basicity and that they exhibited different catalytic activities in

the four solvents. Based on our results, we would like to propose the validity of considering the effect of the interaction between the solvent and catalyst in the preparation of efficient Mg–Al HT catalysts for the isomerization of glucose to fructose.

2. Results and Discussion

2.1. Formation of HTX Catalysts ($X = 1.5, 2, 3, \text{ and } 4$)

We performed XRD measurements to confirm the structural properties of Mg–Al HT catalysts prepared with different Mg/Al atomic ratios. As can be evinced from Figure 2, the HTX catalysts included peaks corresponding to the (003), (006), (009), and (110) planes (JCPDS #14-0191) [46]. These characteristic peaks indicated that the prepared HTX catalysts maintained a well-developed layered double hydroxide structure. In addition, data confirmed that the XRD peaks for the (003) and (110) planes gradually widened as the atomic ratio of Mg/Al decreased, indicating that smaller crystallite size had formed. Therefore, XRD analysis results indicated that Mg–Al HT catalysts characterized by different Mg/Al atomic ratios had been successfully prepared. Notably, furthermore, according to literature, the basic properties of the catalyst are expected to depend on the crystallite sizes [24,38,44].

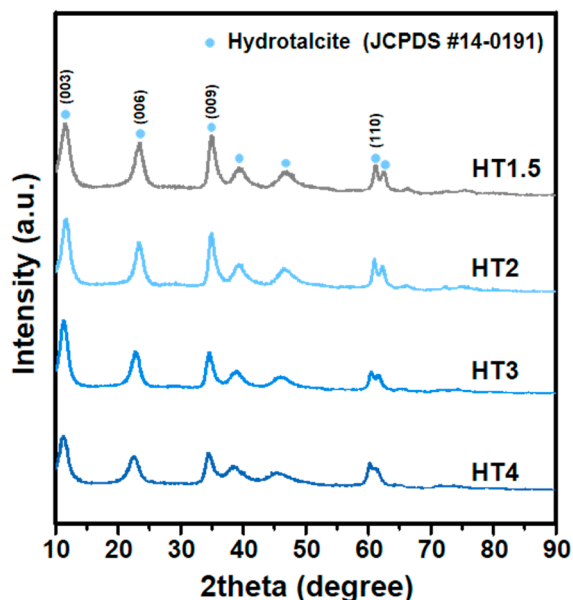


Figure 2. X-ray diffraction (XRD) patterns of the prepared HTX catalysts ($X = 1.5, 2, 3, \text{ and } 4$).

Table 1 showed the measured values for the crystallite size, BET surface area, and Mg/Al atomic ratio of the HTX catalysts. Crystallite sizes were calculated via the Scherrer's equation and using the XRD peaks of the samples for the (003) and (110) planes. As expected based on the XRD measurement results, the crystallite size values of the prepared HTX catalysts displayed a tendency to decrease as the Mg/Al atomic ratio decreased. As previously reported, the decrease in crystallite size as the Mg/Al atomic ratio decreases could be explained by Al centers interrupting the growth of a brucite-like layer structure; please note that brucite is a mineral form of $\text{Mg}(\text{OH})_2$. In other words, HTX catalysts characterized by a low Mg/Al atomic ratio included a relatively high amount of Al^{3+} . As a result, Al^{3+} ions filled sites that would have otherwise been occupied by Mg^{2+} ions, which limited the formation of the layered structure, resulting in the observed decrease in crystallite size. The tendency of the crystallite size to decrease as the Mg/Al atomic ratio decreased was also consistent with the observation of a gradual increase in the BET surface area of the samples.

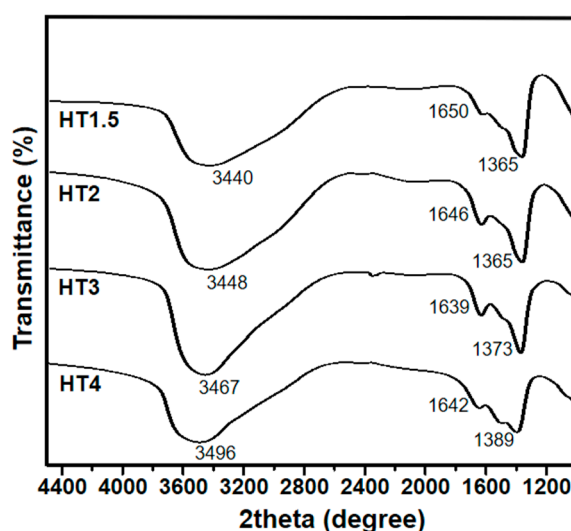
Table 1. Physical properties and chemical composition of HTX (X = 1.5, 2, 3, and 4) catalysts.

Catalyst	Crystallite Size (nm) ^a		S_{BET} (m ² /g) ^b	Mg/Al Ratio ^c
	(003)	(110)		
HT1.5	4.5	11.0	139.6	1.8
HT2	5.1	11.3	105.2	2.1
HT3	5.3	11.4	60.2	2.9
HT4	5.6	12.1	57.9	3.9

^a Crystallite size was calculated by the Scherrer equation. ^b S_{BET} : specific area as calculated using the Braunauer–Emmett–Teller (BET) plot. ^c Chemical composition was determined by inductively coupled plasma atomic emission spectroscopy (ICP-AES) analysis.

We also performed ICP-AES measurements to confirm the successful formation of HTX catalysts, and the relevant results are shown in Table 1. As can be evinced from this, the observed Mg/Al atomic ratios of the prepared samples were slightly higher or similar to the target values. However, it was judged to be somewhat consistent, because all Al species were incompletely integrated into a layered structure. Evidence thus strongly supported the successful formation of HTX (X = 1.5, 2, 3, and 4) catalysts characterized by different Mg/Al atomic ratios. Notably, the basic properties of the catalysts were expected to be controllable through this change in composition [44].

FTIR and FE-SEM analyses were also performed to further confirm the successful formation of HTX catalysts. Figure 3 showed the FTIR spectra of all the catalyst samples. All spectra included the typical peaks of Mg–Al HT, at 3440–3482, 1639–1650, and 1365–1380 cm^{−1} [44]. Among these peaks, the one at about 3450 cm^{−1} shifted to lower wavenumber values as the Mg/Al atomic ratio decreased. This peak appeared to be due to a variety factors, such as interlayer water molecules, stretching vibrations of –OH in the hydroxide layer, positively charged hydroxide layers, and hydrogen bonds between water molecules and anionic species [46–48]. According to this, the peak shifted to lower wavenumber values as the Al content increased (and the Mg/Al atomic ratio decreased), because strong hydrogen bonds were formed [46–48]. These results also corroborated the conclusion that the desired samples had been successfully prepared.

**Figure 3.** Fourier transform infrared (FTIR) spectra of the prepared HTX catalysts (X = 1.5, 2, 3, and 4).

Result of FE-SEM analysis is presented in Figure 4. As can be evinced from this figure, the HTX catalysts maintained their unique double-layer structure. These appeared to be limited to the growth of the layered structure, because Mg²⁺ ions were replaced with Al³⁺ ions due to the increase in the amount of Al³⁺ cations as the Mg/Al atomic ratio decreased. These results were consistent with those of XRD, crystallite size, FT-IR, and BET surface area analyses.

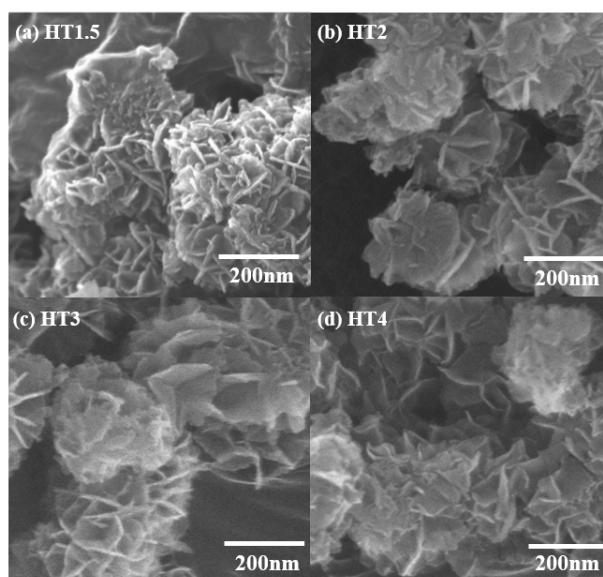


Figure 4. Field emission scanning electron microscopy images (FE-SEM) of the prepared HTX catalysts ($X = 1.5, 2, 3$, and 4): (a) HT1.5, (b) HT2, (c) HT3, and (d) HT4.

2.2. Properties of Various Solvents Used for Glucose Isomerization

We used four polar solvents (water, MeOH, DMSO, and DMF) for the glucose isomerization. In particular, water and MeOH are polar protic solvents, whereas DMSO and DMF are polar aprotic solvents. Literature data indicated that the polarity, basicity, and acidity of the solvent affect the efficiency of glucose conversion to fructose [17,31,49]. Polarity is the property that allows the solvent to stabilize charges or dipoles as a result of dielectric polarization. Basicity represents the ability of the solvent to accept protons, whereas acidity identifies the solvent's ability to provide protons in solvent-to-solvent hydrogen bonding. The effect of solvent has been extensively studied for glucose isomerization [17,28]. In some studies, it has been reported that the role of solvent in the ring-opening is very important and that the barrier of the reaction is a little higher from acidic solution than basicity solution [30]. Other studies have reported that aprotic solvents suppress the overall conversion of glucose, but significantly increase the selectivity of dehydration products during glucose degradation. On the other hand, protic solvents have been reported to have little effect on this decomposition [31]. Table 2 listed the values for the polarity, basicity, and acidity of the four solvents used in this study [50]. As can be evinced, water displayed the highest polarity and acidity among the four solvents. On the other hand, DMSO displayed the highest basicity. We expect that various properties of the solvent influence the basic properties of the catalyst, thus affecting the efficiency of glucose isomerization. Therefore, we performed the glucose isomerization in various solvents over the different prepared HTX catalysts.

Table 2. Properties of four solvents used for the glucose isomerization.

Solvent	π (Polarity)	β (Basicity)	α (Acidity)
Water	1.09	0.18	1.17
MeOH ^a	0.60	0.62	0.93
DMSO ^b	1.00	0.76	0.00
DMF ^c	0.88	0.69	0.00

^a Methanol (MeOH); ^b Dimethyl sulfoxide (DMSO); ^c N,N-dimethylformamide (DMF).

2.3. Glucose Isomerization to Fructose Over HTX Catalysts ($X = 1.5, 2, 3$, and 4)

Glucose isomerization was performed to probe the activity of HTX catalyst in the different solvents. The said reaction was carried out for 5 h in a batch-type reactor at 100 °C. Figure 5 presented values for the glucose conversion, fructose selectivity, and fructose yield of the various reaction with different solvents. The catalytic activities were calculated using the equations from Section 3.4.

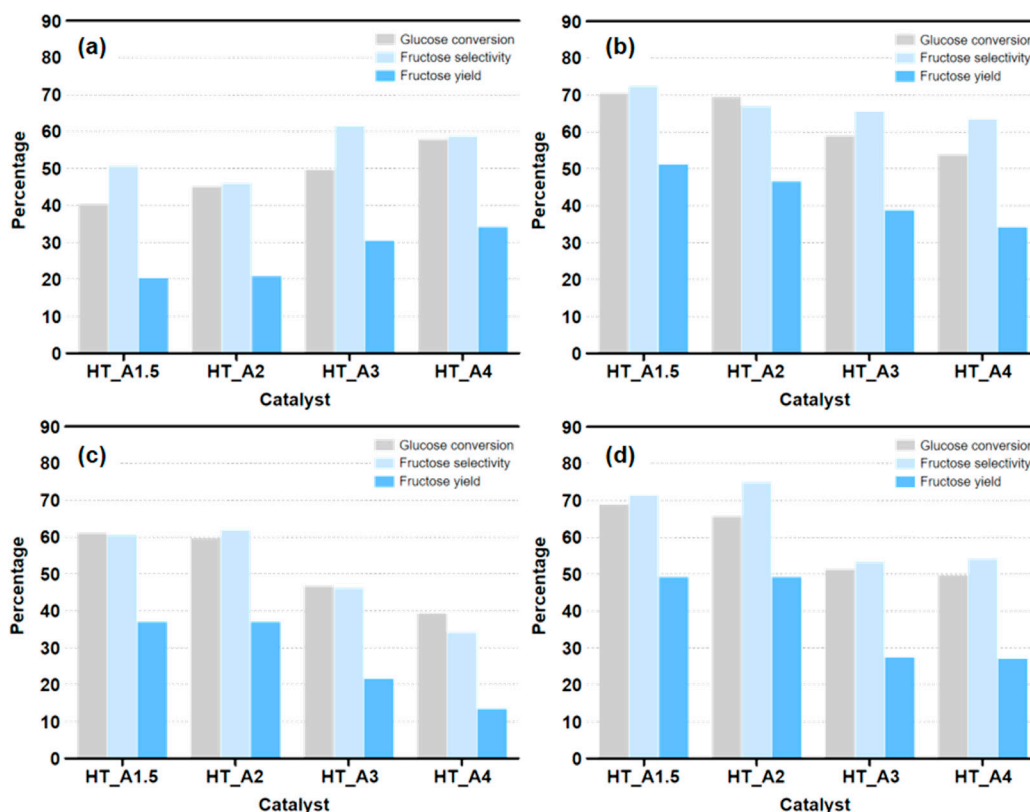


Figure 5. Catalytic activities of HTX catalysts ($X = 1.5, 2, 3$, and 4) in the glucose isomerization. Catalytic activities measured in (a) water, (b) MeOH, (c) DMSO, and (d) DMF.

Results thus confirmed that the activity of each HTX catalyst were different depending on the solvents used in the reaction. When water was used as the solvent, HT4 afforded the highest fructose yield, whereas use of HT1.5 afforded the lowest yield. Additionally, the fructose yield and glucose conversion decreased as the Mg/Al atomic ratio of the catalyst decreased. By contrast, when MeOH, DMSO, and DMF were used as the solvents, HT1.5 afforded the highest fructose yield, whereas HT4 afforded the lowest fructose yield. Contrary to the results obtained in water, when MeOH, DMSO, and DMF were used as solvents in the glucose isomerization, fructose yield and glucose conversion increased as the Mg/Al atomic ratio of the catalyst decreased. As described above, each HTX catalyst displayed a different activity for glucose isomerization. As mentioned earlier, the described activity was expected to depend on the basic properties of the catalysts, which in turn are affected by the solvents used for the isomerization. In order to evaluate this assumption, we determined the base properties of the catalysts, implementing the Hammett indicator method; we compared the base strength exhibited by the HTX catalysts in each solvent.

2.4. The Basic Properties of HTX Catalysts ($X = 1.5, 2, 3$, and 4) in Various Solvents

Among the available methods for analyzing the basic properties of a catalyst, CO₂-TPD analysis allows to determine a catalyst base strength by adsorbing CO₂ gas on the catalyst and then comparing the temperature at which CO₂ is desorbed while increasing the temperature. However, since carbonate

ions present in the intermediate layer of hydrotalcite are released during the described experiment, it is difficult to accurately determine the base strength of HTX catalysts via CO₂-TPD analysis [43]. In addition, we decided that CO₂-TPD analysis was not suitable for this study, because we wanted to analyze the change in basic properties of the catalysts in various solvents. Therefore, we implemented the Hammett indicator method to qualitatively determine the base strengths that the various catalysts displayed in the different solvents.

The results of the Hammett indicator method performed on the various catalysts in the different solvents are presented in Table 3 and Supplementary Materials Figure S1. The data in columns 2–4 of Table 3 provide information on whether the solution characterized by a particular solvent/indicator pair underwent a color change (“O”) or maintained its original color or colorless status (“X”) when a specific HTX catalyst was added to it. In particular, the solvents tested included water, MeOH, DMSO, and DMF, whereas the two indicators utilized were B.T.B and P.P, which have different values of the base strength, $H_- = 7.3$ and $H_- = 9.5$, respectively. Notably, the ‘ H_- ’ parameter is indicative of the relative basic strength of the indicator: A high H_- value means that the indicator has a relatively high base strength. When using B.T.B, a change in color of the solution from yellow to green or blue means that the catalyst has a base strength of 7.3 or higher in the utilized solvent. Similarly, when P.P is used, a change in appearance of the solution from colorless to pink means that the catalyst has a base strength of 9.5 or more in the utilized solvent. Moreover, when using the same solvent/indicator pair, the darker the color of the solution following a color change, the higher the catalyst base strength.

Table 3. Results of Hammett indicator experiments conducted in various solvents.

Indicator/Solvent	Catalyst			
	HT1.5	HT2	HT3	HT4
B.T.B ^a /Water	O ^c	O	O	O
P.P ^b /Water	X ^d	X	O	O
B.T.B/MeOH	O	O	O	O
P.P/MeOH	O	O	X	X
B.T.B/DMSO	O	O	O	O
P.P/DMSO	O	O	X	X
B.T.B/DMF	O	O	O	O
P.P/DMF	O	O	X	X

^a Bromothymol blue (B.T.B); ^b Phenolphthalein (P.P); ^c The color of the indicator changed; ^d The color of the indicator did not change.

Based on the results of the Hammett indicator method, it could be confirmed that the basic properties of HTX catalysts changed depending on the solvent used. First, in the case of the B.T.B/water of indicator/solvent pair, upon the addition of all four catalysts, the solution’s color changed from yellow to green or blue. However, only when HT3 and 4 were added to the solutions characterized by the P.P/water of indicator/solvent pair did the said solutions switch from colorless to pink. This observation indicates that HT3 and 4 had relatively high base strength in water. In addition, the solutions comprising the indicator B.T.B dissolved in MeOH, DMSO, or DMF also changed in color from yellow to green or blue as all four catalysts were added to them. However, in contrast to the results obtained using water as the solvent, the solutions containing indicator P.P dissolved in MeOH, DMSO, or DMF switched from colorless to pink only when catalysts HT1.5 and 2 were added to them. Notably, when HT3 and HT4 were added to these solutions, although the catalysts themselves turned pink, no clear change in the color of the solution was observed. This observation descends from the fact that more than 10% of the indicator should be adsorbed on the base site of the catalyst, but for HT3 and 4 catalysts in MeOH, DMSO, and DMF solvents, there were not enough bases for the indicator to adsorb [51]. So, we determined that the change in color of the solutions containing HT3 and 4 solutions was not substantial enough to be observable. By contrast, HT1.5 and 2 displayed a relatively high base strength in MeOH, DMSO, and DMF.

These results indicated that the prepared HTX catalysts displayed different basic properties in different solvents. Therefore, evidence strongly supported our suggestion that it is not just the individual properties of the solvent and catalyst that should be considered when aiming to improve the efficiency of glucose isomerization to fructose, but also the interaction between solvent and catalyst. We also confirmed together the basic properties of the catalyst with the solvent and the activity of the glucose isomerization that were the result of the Hammett indicator method from the following.

2.5. Relationship between the Fructose Yield and the Catalyst Basic Properties in Various Solvents Used in the Glucose Isomerization

Figure 6 showed the fructose yields and the results of Hammett indicator method performed to investigate the glucose isomerization. The x -axis of each graph presents the catalyst utilized, whereas the fructose yield is reported in the y -axis. For the fructose yield, the average values were used after conducting the glucose isomerization three times. The standard deviation of the experimental values was shown by the red line. The color of the graph reflected the color of the solution when P.P was used in the Hammett indicator method. Additionally, the bar in the right hand side of Figure 6 provided visual information on how the color of the solution reflected the relative base strength: The higher the position of the color in the bar, the higher the base strength of the catalyst.

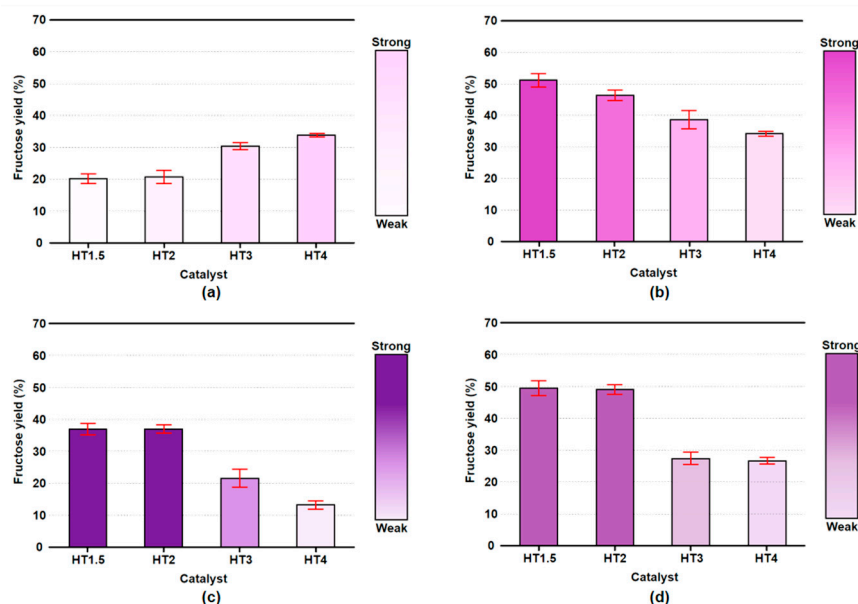


Figure 6. Relationship between fructose yield and the base properties of HTX ($X = 1.5, 2, 3$, and 4) catalysts as determined using the phenolphthalein indicator in various solvents: (a) water, (b) MeOH, (c) DMSO, and (d) DMF.

As mentioned earlier, different HTX catalysts displayed significantly different activities in the glucose isomerization in the same solvent. Furthermore, the activity of a specific catalyst was strongly influenced by the identity of the solvent used for the reaction. In addition, the results of the Hammett indicator method confirmed that the base strength of the catalysts varied depending on the solvent. When water was used as the solvent for the glucose isomerization, HT1.5 displayed relatively weaker base strength than HT2, 3, and 4, and with HT1.5 as the catalyst, the value of fructose yield was the lowest. By contrast, HT4 catalyst displayed the strongest base strength and the highest fructose yield. On the other hand, HT1.5 displayed relatively strong base strength, and its use was associated with the highest fructose yield in MeOH, DMSO, and DMF. Notably, in the mentioned solvents, HT4 displayed relatively weak base strength and its use was associated with low fructose yield. All in all, evidence thus indicates that the fructose yield of the glucose isomerization increased with the base

strength of the catalyst in the reaction solvent, and it decreased as the catalyst base strength decreased. Moreover, results strongly supported our suggestions that the basic properties of the catalyst were strongly influenced by the solvent utilized and that these basic properties could in turn affect the yield of the glucose isomerization.

In summary, when used in the same solvent, the prepared HTX catalysts displayed different base properties. In other words, the basic properties of Mg–Al HT catalysts could be controlled tuning their Mg/Al atomic ratio. In addition, the catalytic activities and the basic properties of the catalysts varied significantly in different solvents used for the glucose isomerization. Our results confirmed that the basic properties of the catalyst depend on the solvent and that changes in the basic properties of the catalyst affect the yield of fructose from glucose isomerization. Therefore, we suggested the validity of evaluating the relationship between the changes in the basic properties of the catalyst caused by the solvent and the solvent, rather than the properties of the catalyst and the solvent considered in isolation, as an approach to increasing the efficiency of the process leading to fructose production via glucose isomerization.

3. Materials and Methods

3.1. Catalyst Preparation

Mg–Al HT catalysts with Mg/Al atomic ratios ranging from 1.5 to 4 were prepared by a co-precipitation method. We used $\text{Mg}(\text{NO}_3)_2 \cdot 6\text{H}_2\text{O}$ (Sigma-Aldrich, St. Louis, MO, USA) and $\text{Al}(\text{NO}_3)_3 \cdot 9\text{H}_2\text{O}$ (Sigma-Aldrich) as metal precursors. To form a metal precursor solution, known amounts of these precursors were dissolved in 100 mL of distilled water [44]. Moreover, in order to obtain a basic solution, known amounts of NaOH (Sigma-Aldrich) and Na_2CO_3 (Sigma-Aldrich) were dissolved in 75 mL of distilled water. This basic solution was used as a precipitator, with its pH acting as a precipitation control agent; notably, the Na_2CO_3 solution was also used as a source of interlayer anions. Thereafter, co-precipitation was performed by pooling together the mentioned two solutions under stirring while the pH was maintained at 9.5 in 100 mL of distillation at room temperature. The mixture was stirred for 18 h, and the precipitate obtained as a result was collected by filtration and washed with distilled water to remove Na^+ and NO_3^- ions. The precipitate thus isolated was dried at 100 °C overnight. The samples were named HTX ($X = 1.5, 2, 3$, and 4), where X represents the Mg/Al atomic ratio in the sample.

3.2. Catalyst Characterization

To determine the crystalline structures of the prepared catalysts, X-ray diffraction (XRD) patterns were recorded using a X'pert-Pro PAN-analytical diffractometer with Cu-K α radiation ($\lambda = 1.54056 \text{ \AA}$). Notably, the diffraction patterns were recorded within the 2θ range 10° – 90° . FTIR spectra were obtained using a Jasco FTIR 460 spectrometer in the 4500 – 1000 cm^{-1} wavenumber range employing the KBr pellet technique. Field emission scanning electron microscope (FE-SEM) images were obtained using a JSM-6700FE-SEM instrument operating at 15 kV. Prior to the FE-SEM analysis, the samples were treated by conducting resin and coating with platinum. Inductively coupled plasma atomic emission spectroscopy (ICP-AES) analyses were conducted to confirm the Mg/Al atomic ratios in the samples using an OPTIMA 4300DV (Perkin-Elmer) instrument. In order to determine the specific surface areas of the catalyst samples via the Brunauer–Emmett–Teller (BET) method, N_2 adsorption and desorption measurements were conducted using a TriStar II (Micromeritics Corp.) instrument.

3.3. Hammett Indicator Method

Several methods exist to analyze the basic properties of catalysts. Among them, CO_2 temperature-programmed desorption (CO_2 -TPD) is widely used to analyze the basic properties of heterogeneous catalysts. However, in the case of the Mg–Al HT catalysts used in this study, it is difficult to obtain accurate data from CO_2 -TPD experiments, given the presence of carbonate ions in

the catalyst's intermediate layer. Therefore, we opted to qualitatively analyze the base properties of the HTX catalysts in various solvents employing the Hammett index titration method, which is widely utilized to macroscopically analyze the acid or base properties of catalysts relying on pH-dependent color changes of the solution.

In order to qualitatively analyze the strength of the basic sites of the samples, two Hammett indicators were utilized: bromothymol blue (B.T.B, $H_a = 7.3$) and phenolphthalein (P.P, $H_a = 9.5$). These indicators were added to the four solvents utilized in this study to obtain 1.0×10^{-5} M solutions. Notably, the four solvents used to carry out the glucose isomerization were water, methanol (MeOH), Dimethyl sulfoxide (DMSO), and N,N-dimethylformamide (DMF). In detail, 0.02 g of the catalyst were added to a 2 mL indicator/solvent pair, and the thus obtained solution was stirred for 2 h until equilibrium was reached. Thereafter, the color of the solution was observed to qualitatively infer the strength of the base site.

3.4. Isomerization of Glucose to Fructose and Product Analysis

In this study, isomerization of glucose to fructose was used as a model reaction, which was conducted in a batch-type reactor [24,38,43,44]. In a typical reaction, glucose (0.3 g, Sigma-Aldrich), catalyst (0.1 g), and solvent (10 mL) were introduced into the reactor, which was then sealed. The reaction was carried out in four solvents: water, MeOH (DUKSAN), DMSO (JUNSEI), and DMF (Sigma-Aldrich). The reactor was placed in a pre-heated oil bath at 100 °C for 5 h, during which the contents of the reactor were subjected to vigorous stirring. After the catalytic reaction, the reactor was immersed in cold water and allowed to cool to room temperature, a process that triggered the precipitation of the catalyst, which was subsequently removed by filtration using a syringe filter. The filtrate was analyzed using high performance liquid chromatography (HPLC) with a refractive index detector (YL9100, Biorad Aminex HPX87H column). The flow rate of the mobile phase (0.005 M H_2SO_4 solution) was fixed at 0.5 mL/min and the temperature of the column (Biorad Aminex HPX87H) was maintained at 50 °C. Glucose conversion, fructose selectivity, and fructose yield are calculated using the following equations.

$$\text{Conversion of glucose (\%)} = \frac{\text{moles of glucose reacted}}{\text{moles of glucose supplied}} \times 100 \quad (1)$$

$$\text{Selectivity for fructose (\%)} = \frac{\text{moles of fructose formed}}{\text{moles of glucose reacted}} \times 100 \quad (2)$$

$$\text{Yield for fructose (\%)} = \frac{\text{moles of fructose formed}}{\text{moles of glucose supplied}} \times 100 \quad (3)$$

4. Conclusions

In this study, we prepared a series of Mg–Al HT catalysts (HTX, X = 1.5, 2, 3, and 4) characterized by different Mg/Al atomic ratios (X) implementing the co-precipitation method; we then used the prepared species to catalyze the fructose-producing glucose isomerization. We utilized four different solvents with different properties (water, MeOH, DMSO, and DMF) to perform the said reaction in a batch-type reactor. It indicated that the catalytic activities of HTX catalysts were substantially affected by the reaction solvent utilized. In water, use of HT4 provided the highest fructose yield: by contrast, use of HT1.5 was associated with the highest fructose yields in the other three solvents. In fact, these results were expected based on the different basic properties of the Mg–Al HT catalysts in the different solvents. In other words, the properties of the reaction solvent strongly affected the base properties of HTX catalysts, which in turn affected their catalytic activity in the glucose isomerization. We went on to implement the Hammett indicator method to determine the basic properties of the catalysts in various solvents. We thus confirmed that basic properties of the HTX catalysts were dramatically different in different solvents. HT4 displayed the strongest base strength in water, whereas HT1.5 displayed the strongest relative base strength in the other three solvents. Ultimately, fructose

yield increased alongside the base strength of the catalyst, which was heavily dependent on the chosen reaction solvent. It means that the basic properties of the HTX catalysts can vary depending on the solvent, and the changed basic properties eventually affect their catalytic activity in the glucose isomerization. Therefore, we came to the conclusion that the interaction between the solvent and the catalyst should be taken into careful consideration when designing efficient Mg–Al base catalysts of the glucose isomerization.

Supplementary Materials: The following are available online at <http://www.mdpi.com/2073-4344/10/11/1236/s1>, Figure S1. Hammett indicator method of prepared HTX catalyst ($X = 1.5, 2, 3$, and 4). (a) Bromothymol blue ($H_- = 7.3$) in water, (b) Phenolphthalein ($H_- = 9.5$) in water, (c) Bromothymol blue ($H_- = 7.3$) in MeOH, (d) Phenolphthalein ($H_- = 9.5$) in MeOH, (e) Bromothymol blue ($H_- = 7.3$) in DMSO, (f) Phenolphthalein ($H_- = 9.5$) in DMSO, (g) Bromothymol blue ($H_- = 7.3$) in DMF, (h) Phenolphthalein ($H_- = 9.5$) in DMF.

Author Contributions: Conceptualization, S.A.; syntheses, S.A., D.K.; perform the experiments, S.A., J.C.; writing—original draft preparation, S.A.; writing—review and editing, S.A., J.C.J.; Supervision, J.C.J. All authors have read and agreed to the published version of the manuscript.

Funding: This research was funded by the Basic Science Research Program through the National Research Foundation of Korea (NRF), grant number 2015R1D1A1A01059724.

Acknowledgments: This research was supported by the Basic Science Research Program through the National Research Foundation of Korea (NRF) funded by the Ministry of Education (No.2015R1D1A1A01059724).

Conflicts of Interest: The authors declare no conflict of interest.

References

- Lucia, L.A.; Argyropoulos, D.S.; Adamopoulos, L.; Gaspar, A.R. Chemicals and energy from biomass. *Can. J. Chem.* **2006**, *84*, 960–970. [CrossRef]
- Hall, D.O.; Scrase, J.I. Will biomass be the environmentally friendly fuel of the future? *Biomass Bioenergy* **1998**, *15*, 357–367. [CrossRef]
- Bridgwater, A.V. Review of fast pyrolysis of biomass and product upgrading. *Biomass Bioenergy* **2012**, *38*, 68–94. [CrossRef]
- Bridgwater, A.V. Production of high grade fuels and chemicals from catalytic pyrolysis of biomass. *Catal. Today* **1996**, *29*, 285–295. [CrossRef]
- Mohammadali, E.N. Effect of reaction temperature and type of catalyst on hydrogen production in supercritical water gasification of biomass. *Iran. J. Energy Environ.* **2012**, *3*, 202–209. [CrossRef]
- Sanders, J.P.M.; Clark, J.H.; Harmsen, G.J.; Heeres, H.J.; Heijnen, J.J.; Kersten, S.R.A.; Swaaij, W.P.M.; Moulijn, J.A. Process intensification in the future production of base chemicals from biomass. *Chem. Eng. Process.* **2012**, *51*, 117–136. [CrossRef]
- Moulijn, J.A.; Stankiewicz, A.; Grievink, J.; Górak, A. Process intensification and process systems engineering: A friendly symbiosis. *Comput. Chem. Eng.* **2008**, *32*, 3–11. [CrossRef]
- Stankiewicz, A.; Moulijn, J.A. Process intensification: Transforming chemical engineering. *Chem. Eng. Prog.* **2000**, *96*, 22–33.
- Lee, S.U.; Jung, K.; Park, G.W.; Seo, C.; Hong, Y.K.; Hong, W.H.; Chang, H.N. Bioprocessing aspects of fuels and chemicals from biomass. *Korean J. Chem. Eng.* **2012**, *29*, 831–850. [CrossRef]
- Cambero, C.; Sowlati, T. Assessment and optimization of forest biomass supply chains from economic, social and environmental perspectives—A review of literature. *Renew. Sustain. Energy Rev.* **2014**, *36*, 62–73. [CrossRef]
- Loipersböck, J.; Lenzi, M.; Rauch, R.; Hofbauer, H. Hydrogen production from biomass: The behavior of impurities over a CO shift unit and a biodiesel scrubber used as a gas treatment stage. *Korean J. Chem. Eng.* **2017**, *34*, 2198–2203. [CrossRef]
- Takagaki, A.; Tagusagawa, C.; Domen, K. Glucose production from saccharides using layered transition metal oxide and exfoliated nanosheets as a water-tolerant solid acid catalyst. *Chem. Commun.* **2008**, *42*, 5363–5365. [CrossRef] [PubMed]
- Huber, G.W.; Iborra, S.; Corma, A. Synthesis of Transportation Fuels from Biomass: Chemistry, Catalysts, and Engineering. *Chem. Rev.* **2006**, *106*, 4044–4098. [CrossRef]

14. Moliner, M.; Román-Leshkov, Y.; Davis, M.E. Tin-containing zeolites are highly active catalysts for the isomerization of glucose in water. *Proc. Natl. Acad. Sci. USA* **2010**, *107*, 6164–6168. [[CrossRef](#)] [[PubMed](#)]
15. Guo, Q.; Ren, L.; Alhassan, S.M.; Tsapatsis, M. Glucose isomerization in dioxane/water with Sn- β catalyst: Improved catalyst stability and use for HMF production. *Chem. Commun.* **2019**, *55*, 14942–14945. [[CrossRef](#)]
16. Qian, X.; Wei, X. Glucose Isomerization to Fructose from ab Initio Molecular Dynamics Simulations. *J. Phys. Chem. B* **2012**, *116*, 10898–10904. [[CrossRef](#)] [[PubMed](#)]
17. Zhang, N.; Meng, X.; Wu, Y.; Song, H.; Huang, H.; Wang, F.; Lv, J. Highly Selective Isomerization of Glucose into Fructose Catalyzed by a Mimic Glucose Isomerase. *ChemCatChem* **2019**, *11*, 2355–2361. [[CrossRef](#)]
18. Yoo, C.G.; Li, N.; Swannell, M.; Pan, X. Isomerization of glucose to fructose catalyzed by lithium bromide in water. *Green Chem.* **2017**, *19*, 4402–4411. [[CrossRef](#)]
19. Souzanchi, S.; Nazari, L.; Rao, K.T.V.; Yuan, Z.; Tan, Z.; Xu, C. Catalytic isomerization of glucose to fructose using heterogeneous solid Base catalysts in a continuous-flow tubular reactor: Catalyst screening study. *Catal. Today* **2019**, *319*, 76–83. [[CrossRef](#)]
20. Roman-Leshkov, Y.; Moliner, M.; Labinger, M.A.; Davis, M.E. Mechanism of glucose isomerization using a solid lewis acid catalyst in water. *Angew. Chem. Int. Ed.* **2010**, *47*, 8954–8957. [[CrossRef](#)]
21. Tewari, Y.B. Thermodynamics of industrially-important, enzyme-catalyzed reactions. *Appl. Biochem. Biotechnol.* **1990**, *23*, 187–203. [[CrossRef](#)] [[PubMed](#)]
22. Lima, S.; Dias, A.S.; Lin, Z.; Brandão, P.; Ferreira, P.; Pillinger, M.; Rocha, J.; Calvino-Casilda, V.; Valente, A.A. Isomerization of d-glucose to d-fructose over metallosilicate solid bases. *Appl. Catal. A* **2008**, *399*, 21–27. [[CrossRef](#)]
23. Hattori, H. Basic catalysts and fine chemicals. *Stud. Surf. Sci. Cat.* **1993**, *78*, 35–49. [[CrossRef](#)]
24. Yu, S.; Kim, E.; Park, S.; Song, I.K.; Jung, J.C. Isomerization of glucose into fructose over Mg–Al hydrotalcite catalysts. *Catal. Commun.* **2012**, *29*, 63–67. [[CrossRef](#)]
25. Hattori, A.; Hattori, H.; Tanabe, K. Double-bond migration of allylamine to enamine over basic oxide catalysts. *J. Catal.* **1980**, *65*, 245–252. [[CrossRef](#)]
26. Kumar, S.; Nepak, D.; Kansal, S.K.; Elumalai, S. Expeditious isomerization of glucose to fructose in aqueous media over sodium titanate nanotubes. *RSC Adv.* **2018**, *53*, 30106–30114. [[CrossRef](#)]
27. Zhao, S.; Guo, X.; Bai, P.; Lv, L. Chemical Isomerization of Glucose to Fructose Production. *Asian J. Chem.* **2014**, *26*, 4537–4542. [[CrossRef](#)]
28. Yabushita, M.; Shibayama, N.; Nakajima, K.; Fukuoka, A. Selective Glucose-to-Fructose Isomerization in Ethanol Catalyzed by Hydrotalcites. *ACS Catal.* **2019**, *9*, 2101–2109. [[CrossRef](#)]
29. Ju, Z.; Zhang, Y.; Zhao, T.; Xiao, W.; Yao, X. Mechanism of Glucose–Fructose Isomerization over Aluminum-Based Catalysts in Methanol Media. *ACS Sustain. Chem. Eng.* **2019**, *7*, 14962–14972. [[CrossRef](#)]
30. Qian, X. Free Energy Surface for Brønsted Acid-Catalyzed Glucose Ring-Opening in Aqueous Solution. *J. Phys. Chem. B* **2013**, *117*, 11460–11465. [[CrossRef](#)]
31. Song, B.; Wu, Z.; Yu, Y.; Wu, H. Hydrothermal Reactions of Biomass-Derived Platform Molecules: Distinct Effect of Aprotic and Protic Solvents on Primary Decomposition of Glucose and Fructose in Hot-Compressed Solvent/Water Mixtures. *Ind. Eng. Chem. Res.* **2020**, *59*, 7336–7345. [[CrossRef](#)]
32. Graça, I.; Iruetagoien, D.; Chadwick, D. Glucose isomerisation into fructose over magnesium-impregnated NaY zeolite catalysts. *Appl. Catal. B Environ.* **2017**, *206*, 434–443. [[CrossRef](#)]
33. Ohyama, J.; Zhang, Y.; Satsuma, A.; Ito, J. Glucose Isomerization Using Alkali Metal and Alkaline Earth Metal Titanates. *ChemCatChem* **2017**, *9*, 2864–2868. [[CrossRef](#)]
34. Asakawa, M.; Shrotri, A.; Kobayashi, H.; Fukuoka, A. Solvent basicity controlled deformylation for the formation of furfural from glucose and fructose. *Green Chem.* **2019**, *21*, 6146–6153. [[CrossRef](#)]
35. Marianou, A.A.; Michailof, C.M.; Pineda, A.; Iliopoulou, E.F.; Triantafyllidis, K.S.; Lappas, A.A. Glucose to Fructose Isomerization in Aqueous Media over Homogeneous and Heterogeneous Catalysts. *ChemCatChem* **2016**, *8*, 1100–1110. [[CrossRef](#)]
36. Debecker, D.P.; Gaigneaux, E.M.; Busca, G. Exploring, Tuning, and Exploiting the Basicity of Hydrotalcites for Applications in Heterogeneous Catalysis. *Chem. Eur. J.* **2009**, *15*, 3920–3935. [[CrossRef](#)]
37. Othman, M.R.; Helwani, Z.; Martunus, F.W.J.N. Synthetic hydrotalcites from different routes and their application as catalysts and gas adsorbents: A review. *Appl. Organomet. Chem.* **2009**, *23*, 335–346. [[CrossRef](#)]
38. Lee, G.; Kang, J.Y.; Yan, N.; Suh, Y.-W.; Jung, J.C. Simple preparation method for Mg–Al hydrotalcites as base catalysts. *J. Mol. Catal. A Chem.* **2016**, *423*, 347–355. [[CrossRef](#)]

39. Zhang, H.; Shen, Z.; Liang, X. The novel efficient catalyst for biodiesel synthesis from rapeseed oil. *Kinet. Catal.* **2014**, *55*, 293–298. [CrossRef]
40. Jyothi, T.M.; Raja, T.; Sreekumar, K.; Talawar, M.B.; Rao, B.S. Influence of acid-base properties of mixed oxides derived from hydrotalcite-like precursors in the transfer hydrogenation of propiophenone. *J. Mol. Catal. A Chem.* **2000**, *157*, 193–198. [CrossRef]
41. Climent, M.J.; Corma, A.; Iborra, S.; Epping, K.; Velty, A. Increasing the basicity and catalytic activity of hydrotalcites by different synthesis procedures. *J. Catal.* **2004**, *225*, 316–326. [CrossRef]
42. Moreau, C.; Durand, R.; Roux, A.; Tichit, D. Isomerization of glucose into fructose in the presence of cation-exchanged zeolites and hydrotalcites. *Appl. Catal. A Gen.* **2000**, *193*, 257–264. [CrossRef]
43. Kwon, D.; Kang, J.Y.; An, S.; Yang, I.; Jung, J.C. Tuning the base properties of Mg–Al hydrotalcite catalysts using their memory effect. *J. Energy Chem.* **2020**, *46*, 229–236. [CrossRef]
44. Kang, J.Y.; Lee, G.; Suh, Y.-W.; Jung, J.C. Effect of Mg/Al Atomic Ratio of Mg–Al Hydrotalcites on Their Catalytic Properties for the Isomerization of Glucose to Fructose. *J. Nanosci. Nanotechnol.* **2017**, *17*, 8242–8247. [CrossRef]
45. Li, C.; Wang, Y.; Zhang, Y.; Wang, M.; Sun, X.; Cui, H.; Xie, Y. Isomerization Kinetics of Glucose to Fructose in Aqueous Solution with Magnesium–Aluminum Hydrotalcites. *Chem. Select* **2020**, *5*, 270–279. [CrossRef]
46. Frost, R.L.; Lopez, A.; Scholz, R.; Sampaio, N.P.; De Oliveira, F.A. SEM, EDS and vibrational spectroscopic study of dawsonite $\text{NaAl}(\text{CO}_3)(\text{OH})_2$. *Spectrochim. Acta Part A Mol. Biomol. Spectrosc.* **2015**, *136*, 918–923. [CrossRef]
47. Frost, R.L.; Spratt, H.J.; Palmer, S.J. Infrared and near-infrared spectroscopic study of synthetic hydrotalcites with variable divalent/trivalent cationic ratios. *Spectrochim. Acta Part A Mol. Biomol. Spectrosc.* **2008**, *72*, 984–988. [CrossRef]
48. Newman, S.P.; Jones, W.; O'Connor, P.; Stamires, D.N. Synthesis of the 3R2 polytype of a hydrotalcite-like mineral. *J. Mater. Chem.* **2002**, *12*, 153–155. [CrossRef]
49. Dyson, P.J.; Jessop, P.G. Solvent effects in catalysis: Rational improvements of catalysts via manipulation of solvent interactions. *Catal. Sci. Technol.* **2016**, *6*, 3302–3316. [CrossRef]
50. Kamlet, M.J.; Abboud, J.L.M.; Abraham, M.H.; Taft, R.W. Linear solvation energy relationships. 23. A comprehensive collection of the solvatochromic parameters, π^* , α , and β , and some methods for simplifying the generalized solvatochromic equation. *J. Org. Chem.* **1983**, *48*, 2877–2887. [CrossRef]
51. Kozo, T.; Tsutomu, Y.; Tsuneichi, T. Solid bases and their catalytic activity. *J. Res. Inst. Catal. Hokkaido Univ.* **1968**, *16*, 425–447.

Publisher's Note: MDPI stays neutral with regard to jurisdictional claims in published maps and institutional affiliations.



© 2020 by the authors. Licensee MDPI, Basel, Switzerland. This article is an open access article distributed under the terms and conditions of the Creative Commons Attribution (CC BY) license (<http://creativecommons.org/licenses/by/4.0/>).